International Journal of Applied Engineering Research
ISSN 0973-4562 Volume 10, Number 4 (2015) pp. 9865-9875

http://www.ripublication.com

Characterization of $(MoO_3)_x$ - $(WO_3)_{1-x}$ Composites

Ch. Prameela and K. Srinivasarao*

Department of Science and Humanities,
Vignan University (*VFSTR University), Vadlamudi - 522 213,*
Andhra Pradesh, India.
[1]* *Corresponding author Email: kotarisrinu@yahoo.co.in*
Phone: 09703824800 Fax: +91(0)863-2534468

Abstract

Here we report the structural properties of $(MoO_3)_x$- $(WO_3)_{1-x}$ composites for various values of x varying from 0 to 1. The XRD reveals that the pure WO_3 crystallises in monoclinic phase and MoO_3 in orthorhombic phase. The individual crystal structures of the oxides were retained even they were as the composite, except the variation in peak intensities. The XRD also reveals that the substance which is having more quantity in the composite is showing high intensity and vice-versa. The grain sizes of WO_3 were decreasing with increasing MoO_3 content in composite. The Raman spectra of pure WO_3 exhibit the peaks at 804, 714, 326, 270, 132 and 70 cm^{-1} and were assigned to various vibration modes of WO_3. By the addition of MoO_3 a small shift in the Raman bands were observed. Raman modes of both MoO_3 and WO_3 were observed when they are approximately in equal compositions, i.e. for x = 0.4. With further increase in MoO_3 content in composite, Raman modes corresponding to MoO_3 with increase in intensity were observed. The IR peaks of pure WO_3 were observed at 591, 548, 533, 518, 501, 487, 471, 455, 441, 427, 424, 418, 403 cm^{-1} and were due to various vibrational modes of WO_3. These modes were observed to be shifting with increasing MoO_3 content. For x = 0.8 the MoO_3 content is more and the most of the IR peaks were correspond to MoO_3 along with few peaks related to WO_3.

Keywords: WO_3, MoO_3, mixed oxide, characterization.

INTRODUCTION

Among the transition metal oxides WO_3 and MoO_3 have been investigated most extensively and their interesting physical properties, makes them suitable for photochromic and electro chromic device applications. These materials show fast response times for application of electric fields, coloration efficiencies, long lifetimes,

etc. due to these properties these materials have been used for information display, sensor devices and the development of smart window [1, 2]. WO_3 is a n-type semi-conductor, has been the most extensively studied material due to its electrochromic properties in the visible and IR region, high-coloration efficiency and relatively low price [3]. WO_3 exhibits multiple polymorphs such as tetragonal (α) [4], orthorhombic (β) [5], monoclinic (ε and γ) [6], triclinic (δ) [7, 8] and so–called pseudo cubic [9]. Each of these forms exhibits different electrical, optical and magnetic behaviours which are favourable for particular applications.

The electronic property is determined by the ability of tungsten ions to change their valence state upon reduction/oxidation processes both in the bulk and at the surface of crystalline grains. In stoichiometric WO_3, the tungsten ions have the valence state 6+ with the 5*d* shell being empty. Depending on the reduction method, the W^{5+}colorcenters can be found in the bulk or at the surface of crystalline grains. Moreover, depending on the concentration of such centers, the additional 5*d* electron can be localized or delocalized on few or infinite number of tungsten ions [10].

The MoO_3 is another n-type semiconducting oxide with orthorhombic layered structure. The layered structure of MoO_3 consists of two octahedra sheets composed of edge-sharing octahedral units, which have six oxygen ions and one molybdenum ion on their vertex and at their center, respectively [11]

Mixed WO_3-MoO_3 based oxide systems are interesting due to the possibility to combine the advantages of the single components properties. Electrochromic MoO_3 has an absorption band close to the maximum of human eye sensitivity. Due to the presence of electronic W^{5+}, W^{6+} states, and the corresponding lower energy states of Mo, WO_3-MoO_3 based oxide systems exhibit stronger optical absorption [12].MoO_3 - WO_3 gas sensors have been shown to be sensitive to O_2. It was shown that the material exhibited n-type conduction behaviour.

In the present study, our aim is to know how the physical properties such as structural, Raman and IR properties of Tungsten trioxide were changed by adding molybdenum trioxide at different compositions.

EXPERIMENTAL

Pure WO_3 powder (purity of 99.99 %) and MoO_3 powder (purity of 99.99 %) is used to prepare different compositions of $(MoO_3)_x$- $(WO_3)_{1-x}$ for x=0, 0.2, 0.4, 0.6, 0.8. Pure WO_3 and various compositions of MoO_3, WO_3 powders have been taken in the mortar and grind well to get fine powders of the mixed oxide and they were sintered at 450 ^{0}C. The structure of the various composites was performed by X-ray diffractometer (Philips PW1830) and the diffraction patterns were collected in the 2θ range from 10º to 80º. CuK_αtarget is used as the X-ray source (λ = 1.542 A°) and the target is operated at 40KV and at 30mA. Raman spectra were recorded in the region of 0 to 2000 cm^{-1}. IR transmission spectra of composites were performed by FT-IR Spectrophotometer (JASCO FTIR-6300) in the range 400 to 1000 cm^{-1}.

RESULTSAND DISCUSSION

XRD

For pure WO_3 and $(MoO_3)_x$ - $(WO_3)_{1-x}$ $0<x<1$ The X-ray diffraction spectra of the $(MoO_3)_x$ - $(WO_3)_{1-x}$composites have been studied to understand their crystallographic structure and were shown in fig.1 respectively. For pure WO_3 the peaks were observed around $2\theta = 23.16^0$, 23.63^0, 24.38^0, 26.62^0, 28.95^0, 33.30^0, 33.62^0, $34.19^0$and these are due to (0 0 2), (0 2 0), (2 0 0), (1 2 0), (1 1 2), (0 2 1), (2 0 1), (2 2 0) orientations which corresponds to monoclinic phase [13-16, JCPDS-00-005-0363].

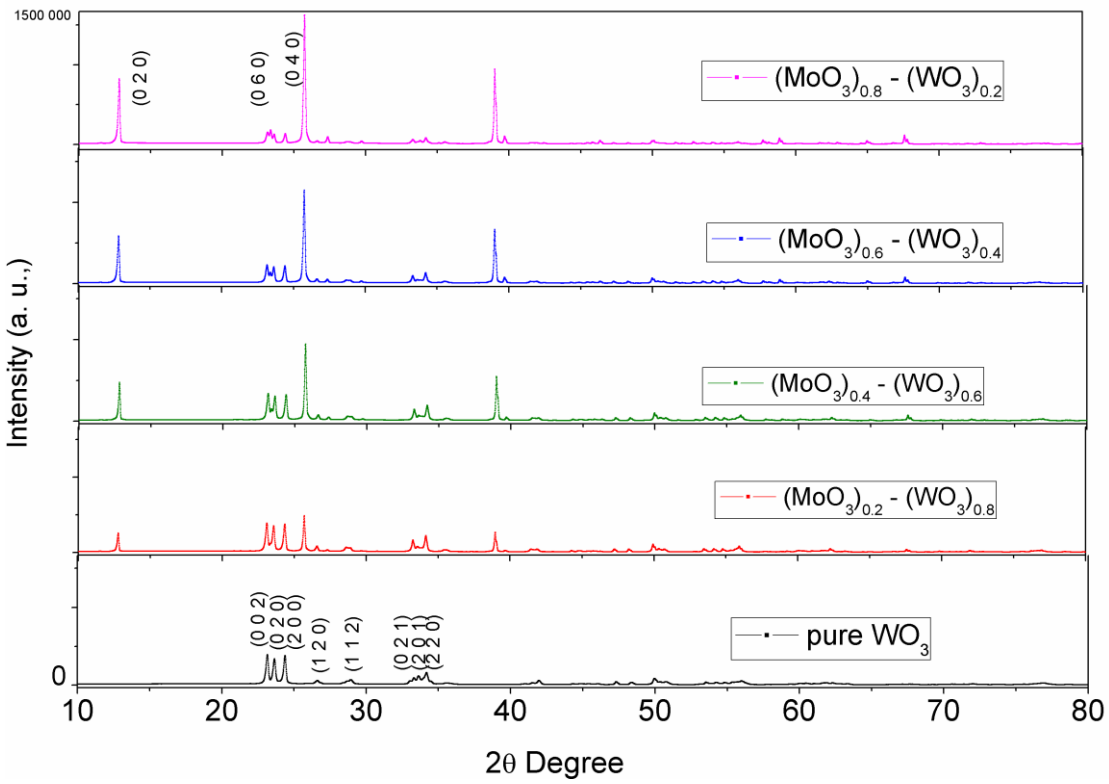

Fig. 1 XRD Spectra of $(MoO_3)_x$- $(WO_3)_{1-x}$ for $0<x<1$.

With the addition of MoO_3 to WO_3 [$(MoO_3)_{0.2}$- $(WO_3)_{0.8}$] the structure remains same but showed reduction in XRD peak intensities. At the same time the low intensity peaks corresponding to orthorhombic MoO_3 were observed. This indicates the individual crystallographic states of the two oxides were unaltered even after the formation of the composite. With the further increment of addition of MoO_3 to WO_3 the peak intensities of (0 0 2), (0 2 0), (2 0 0) orientations corresponds to WO_3 were decreasing and the intensities of the MoO_3 peaks are increasing. For x= 0.8 the composite [$(MoO_3)_{0.8}$ - $(WO_3)_{0.2}$] yields the peaks at $2\theta = 12.8^0$, 25.77^0, 39.02^0 and these are due to (0 2 0), (0 4 0), (0 6 0) orientations [17, 18]. The results were good agreement with the JCPDS file(00-005-0508) of MoO_3 and WO_3.

The grain sizes of high intensity peaks were evaluated using Scherrer's relation

$$L = K\lambda/\beta\cos\theta$$

Where K is constant with a value of about 0.9, λ is the X-ray wavelength (1.54 A^0 for Cu K_α), β the full width at half maximum intensity of the peaks measured in radians and θ is the angle of the diffraction peak (degrees).

There is no significant variation in the grain size of MoO_3 for x = 0.2, 0.4, 0.8 when it is in composite. But for x = 0.6 the grain is decreased significantly. The grain sizes were given in table.1. The growth of (110) orientation was also observed with increasing MoO_3 content in WO_3, which also corresponds to orthorhombic structure of MoO_3. The peak intensity of (1 1 0) is increasing with increasing MoO_3 composition in WO_3. In case of WO_3 the grain sizes as well as crystallographic peak intensities were decreasing with increasing MoO_3 in $(MoO_3)_x - (WO_3)_{1-x}$ [19].Variation of Grain size with composition for $(MoO_3)_x$ - $(WO_3)_{1-x}$ where 0<x<1 was given in Fig. 2.

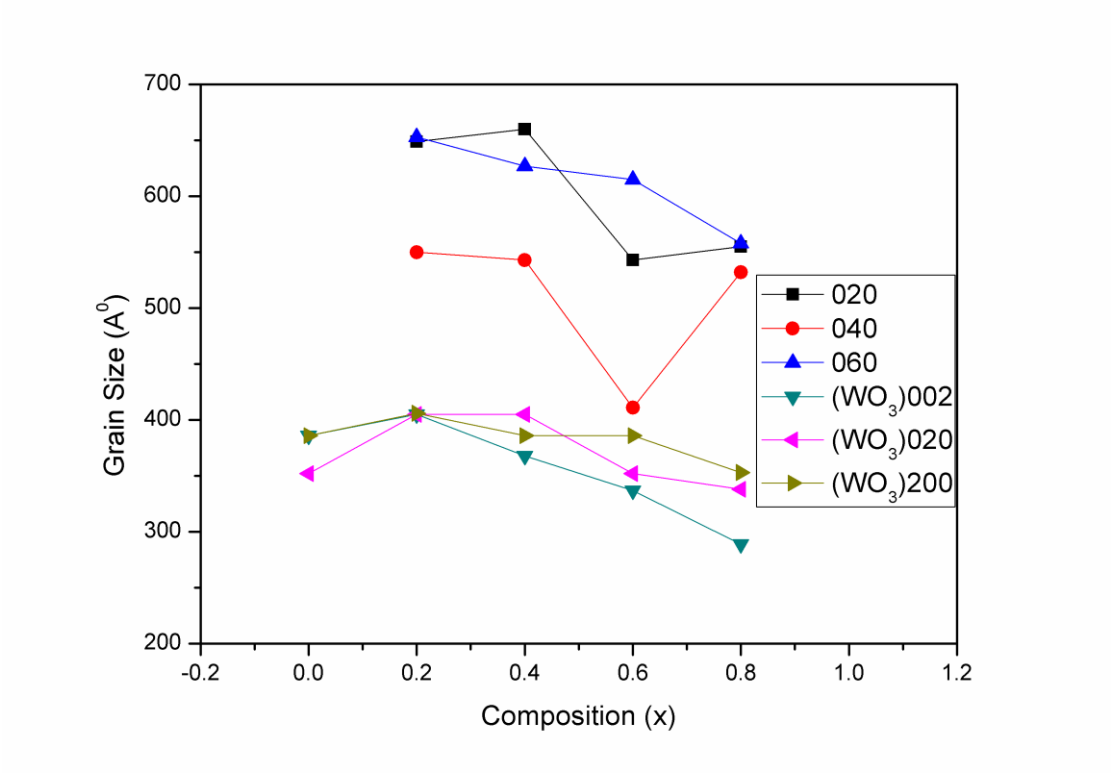

Fig.2 Variation of Grain size with composition for $(MoO_3)_x$- $(WO_3)_{1-x}$ where 0<x<1.

Table1. Grain sizes of $(MoO_3)_x$- $(WO_3)_{1-x}$ for 0<x<1.

Composition (x)	Grain Size (A^0)					
	Crystallographic orientation					
	(0 2 0)	(0 4 0)	(0 6 0)	(0 0 2)	(0 2 0)	(2 0 0)
0	-----	-----	------	386	352	386
0.2	649	550	653	405	405	406
0.4	660	543	627	368	405	386
0.6	543	411	615	337	352	386
0.8	555	532	558	289	338	353

RAMAN

The Raman spectra of $(MoO_3)_x$– $(WO_3)_{1-x}$ for 0<x<1 was studied to understand the vibrational modes of MoO_3 and WO_3 molecules as individuals and as mixers and were shown in fig. 3.

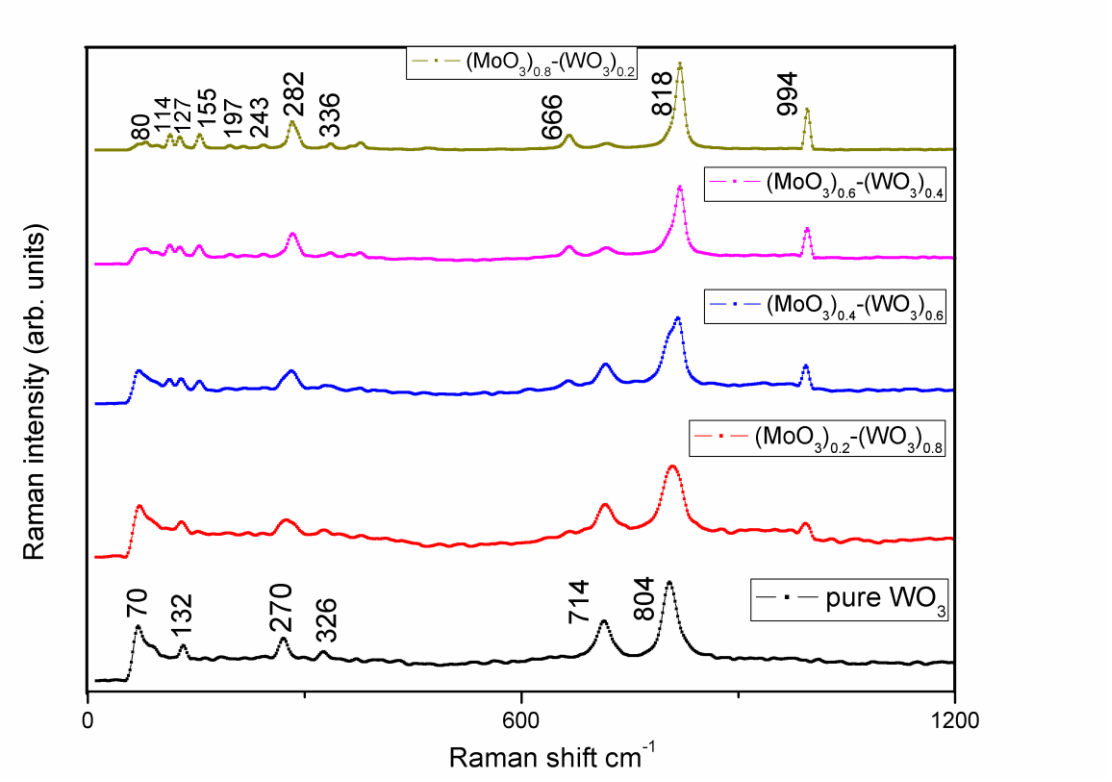

Fig.3 Raman Spectra of $(MoO_3)_x$- $(WO_3)_{1-x}$ for 0<x<1.

For pure WO_3 (x=0) the Raman bands were observed at 804, 714, 326, 270, 132 and 70 cm^{-1}. The sharp peak at 804 cm^{-1} [20, 21] assigned to the $\nu(O\text{-}W^{6+}\text{-}O)$

stretching mode and 714cm^{-1} assigned to the ν(O-W-O) mode and the weak band at 326 cm^{-1} [13, 20] correspond to the vibration of the O-W^{5+}-O and 270 cm^{-1} are due to the bending vibration δ(O-W-O) [21]. The Raman bands at 132 and 70 cm^{-1} were attributed to lattice modes [13].These results were in good agreement with the Raman peaks reported for a monoclinic WO_3 [22].

When MoO_3 (x=0.2) is added to WO_3a single Raman peak corresponding to MoO_3 was observed along with the WO_3 peaks but with a slight shift in the peak positions. The Raman band at 993 cm^{-1}represents the stretching vibration of MoO_3 [23].

With increasing MoO_3 composition (x =0.4) in $(MoO_3)_x$-$(WO_3)_{1-x}$ the peaks observed were 993, 936, 816, 716, 665, 611, 377, 328, 282, 154, 129, 113, 71 cm^{-1}. The Raman peaks observed around 936, 816 cm^{-1} were stretching vibrations and 282 cm^{-1} correspond to bending vibrations of Mo-O bond[24] of orthorhombic MoO_3. The small peak at 716 cm^{-1} is corresponding to W-O stretching vibration of WO_3 [25] and 665 cm^{-1} is of stretching vibrations of α-MoO_3. The weak bands below 200 cm^{-1}are assigned to mixed lattice modes of MoO_3 and WO_3 [26]. With further increasing MoO_3 (at x=0.6) in WO_3 the intense peaks of MoO_3 were dominated and the peaks corresponding to WO_3 were weak due to small percentage of WO_3composition in mixer.

For x = 0.6 the last composition the predominant bands were related to MoO_3 with orthorhombic α-MoO_3 phases [27] which were represented in a table 2.

Table.2. Raman bands of $(MoO_3)_{0.8}$- $(WO_3)_{0.2}$

$(MoO_3)_{0.8}$- $(WO_3)_{0.2}$	Observed	Previous result [9]
	80(s)	82
	114(m)	115
	127(w)	129
	155(m)	158
	197(w)	198
	243	245
Bending(Mo-O)	282(m)	283
	336(m)	337
	468(w)	471
Stretching(Mo_3-O)	666(w)	667
Stretching(Mo_2-O)	818(vs)	819
Stretching(Mo^{6+}=O)	994(s)	995

85-250 skeletel mode, w = weak, m = medium, s = strong, vs = very strong

INFRARED

The Infrared spectra recorded in the wave number range 400-1000 cm^{-1} for pure WO_3 and $(MoO_3)_x$ - $(WO_3)_{1-x}$ for 0<x<1 are shown in fig. 4 respectively.

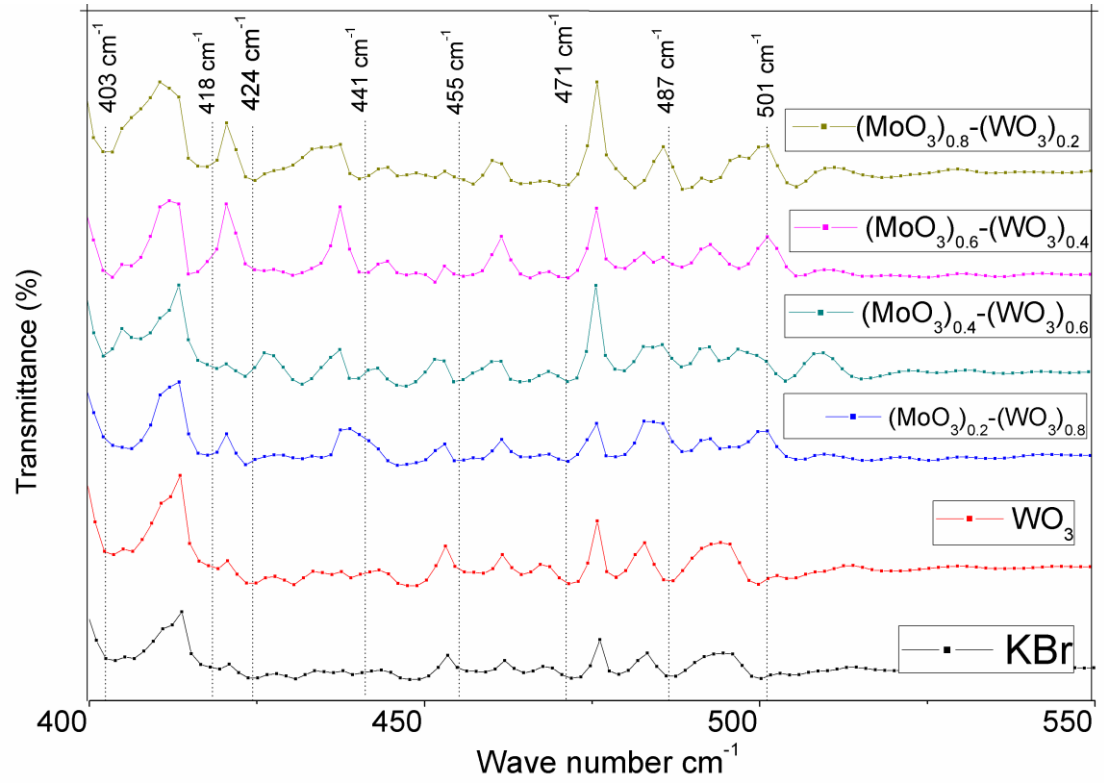

Fig. 4 IR Spectra of $(MoO_3)_x$- $(WO_3)_{1-x}$ for 0<x<1.

In the IR spectrum of mixed oxides, the absorption band between 600 and 1000 cm^{-1} becomes flat and featureless. Such spectra with no characteristic vibrations at typical frequencies could result from a changed configuration of chemical bonds, the vibration modes of which are not IR active [28].

For pure WO_3 the IR peaks were observed at 591, 548, 533, 518, 501, 487, 471, 455, 441, 427, 424, 418, 403 cm^{-1}. WO_3 consists of packed corner-sharing WO_6 octahedra. The corresponding tungsten oxide vibrations are characterized by three infrared regions 900–600 cm^{-1}, 400–200 cm^{-1}, <200 cm^{-1}, which corresponds respectively to (O–W–O) stretching, bending and lattice modes. Shoulder or weak bands are observed in the infrared spectrum at 418 cm^{-1}, and is due to a W-O-W mode of the hexagonal arrangement in h-WO_3 [29]. The band seen at 591 cm^{-1} related to the deformation mode of W-O in WO_3 [30]. The two weak bands at 800 and 589 cm^{-1} superimposed on the broad featureless absorption band in the 1000–500 cm^{-1} region arise from the υ $(W–O_{intra}–W)$ and υ $(W–O_{inter}–W)$ $_{bridging}$ stretching frequencies, respectively [31].

By adding MoO_3 (x = 0.2) to WO_3 the band position of 591 cm^{-1} shifted to lower side and this shifting further continues with increasing MoO_3 percentage in WO_3. In the similar way the band positions were shifted for the other bands also by increasing MoO_3 composition in WO_3. The bands observed at 418, 475 cm^{-1} are related to MoO_3-WO_3. The FTIR study confirms the presence of monoclinic WO_3 and

reveals the influence of the MoO_3 fraction on the spectra [12]. In $(MoO_3)_{0.6}$ - $(WO_3)_{0.4}$ the band at 559 cm^{-1} related to transverse optical vibrational mode of MoO_3 [32]. The band at 558 cm^{-1} related to transverse optical vibrations of Mo-O-Mo [33].

For x=0.8 [$(MoO_3)_{0.8}$ - $(WO_3)_{0.2}$] the bands were observed at 589, 579, 535, 518, 505, 440, 417 cm^{-1}. The bands at 589, 440, 417cm^{-1} were related to WO_3 and the remaining bands were attributed to the Mo = O bond stretching of MoO_3. The bands in the range 500-600 cm^{-1} can be assigned to the Mo-O bond, the strong band at 493 cm^{-1} was assigned to O-Mo-O vibrations [34]. IR spectrum of MoO_3 band at 579 cm^{-1} is assigned to the bending Mo-O-Mo bond vibration [32, 35]. Since this band is present in the spectrum of MoO_3, we connect this to vibrations of Mo-O bond and consider this as an evidence of a MoO_3 fraction in the mixed oxide formed mainly of WO_3[28]. The terminal oxygen symmetry stretching mode (υ_s) of Mo=O and the bridge oxygen asymmetry and symmetry stretching modes ($\upsilon_{as}$and υ_s) of Mo-O-Mo is at 579 cm^{-1} [36].

CONCLUSIONS

The XRD spectra of mixed oxide revealed the individual crystallographic states of the two oxides. In case of WO_3 the grain sizes as well as crystallographic peak intensities were decreasing with increasing MoO_3 in $(MoO_3)_x$ - $(WO_3)_{1-x}$. From the Raman and IR studies we observed that modes of vibrations of WO_3 were shifted by addition of MoO_3 in $(MoO_3)_x$ - $(WO_3)_{1-x.}$

ACKNOWLEDGEMENTS

The authors are thankful to sophisticated analytical instrument facility (SAIF), IIT Madras, Chennai for Raman, S. N. Bose national centre for basic sciences, Kolkata for XRD, Chalapathi institute of pharmaceutical sciences, Guntur, AP for providing IR measurement facility.

References:

1. Yang , Y. A., Cao, Y. W., Loo, B. H., and Yao, J. N., 1998, "Microstructures of Electrochromic MoO_3 Thin Films Colored by Injection of Different Cations, "J. Phys. Chem. B, 102(47), pp. 9392–9396.

2. Manno, D., Serra, A., Giulio, M. D., Micocci, G., and Tepore, A., 1998, "Physical and structural characterization of tungsten oxide thin films for NO gas detection, ".Thin solid films, pp. 324, 44-51.

3. Korosec, R. C., andBukovec, P., 2006, "Sol-Gel prepared NiO thin films for electrochemical applications, " ActaChim. Slov, 53, pp. 136-147.

4. Kehl, W. L., Hay, R. G., and Wahl, D., 1952, "The structure of tetragonal TungstenTrioxide, " J. Appl. Phys, 23, pp. 212-215.

5. Salje, E. K. H., 1977, "The orthorhombic phase of WO_3, "ActaCrystallogr B, 33(2), pp. 574.

6. Salje, E. K. H., Rehmann, S., Pobell, F., Morris, D., and Knight, K. S., 1977, "Crystal structure and paramagnetic behaviour of ε-$WO_{3-x,}$ ". J Phys-Condens Mat, 9, pp. 6563.
7. Woodward, P. M., Sleight, A. W., and Vogt, T., 1995, "Structure refinement of triclinic tungsten trioxide, " J PhysChem Solids, 56, pp. 1305-1315.
8. Diehl, R., Brandt, G., andSalje, E. K. H., 1978, "The crystal structure of triclinic $WO_{3,}$ "ActaCrystallogr B, 34, pp. 1105-1111.
9. Jimenez, I., Arbiol, J., Dezanneau, G., Cornet, A., andMorante, J. R., 2003, "Crystalline structure, defects and gas sensor response to NO_2 and H_2S of tungsten trioxide nanopowders, " Sensors Actuators B: Chem., 93, pp. 475-485.
10. Kuzmin, A., Purans, J., Cazzanelli, E., Vinegoni, C., andMariotto, G., 1998, "X-ray diffraction, extended x-ray absorption fine structure and raman spectroscopy studies of WO_3 powders and (1-x)WO_{3-y}.xReO_2 mixtures, " Journal of applied Physics, 84, pp. 5515-5524.
11. Itoh, T., Matsubara, I., Shin, W., and Izu, N., 2006, "Highly adhesive layered molybdenum oxide thin films prepared on a silicon substrate using suitable buffer materials. Thin solid films, "515, pp. 2709-2716.
12. Ivanova, T., Gesheva, K. A., Abrashev, M., Sharlandjiev, P., andNazarova, D., 2010, "Optical and vibrational spectra analysis of CVD-mixed oxide films: optimization of the films elecrochromic performance, " Journal of Physics: Conference Series, 223(012039), pp. 1-5.
13. Lethy, K. J., Beena, D., Kumar, R. V., Pillai, V. P. M., Ganesan, V., and Sathe, V., 2008, "Structural, optical and morphological studies on laser ablated nanostructured WO_3 thin films, " Applied Surface Science, 254, pp. 2369-2376.
14. Siva Kumar, R., Gopalakrishnan, R., Jayachandran, M., and Sanjeeviraja, C., 2007, "Preparation and characterization of electron beam evaporated WO_3 thin films, " Optical materials, 29, pp. 679-687.
15. Sharma, S., Tomar, M., Puri, N. K., and Gupta, V., 2014, "NO_2 sensing properties of WO_3 thin films deposited by Rf-Magnetron sputtering, " Conference Papers in Science, 683219, pp. 1-5.
16. Maric, R., Wang, Y., and Jain, R., 2014, "Tuning of WO_3 phase transformation and structural modification by reactive spray deposition technology, " J Nanotech Smart Mater, 1, pp. 1-7.
17. Bouzidi, A., Benramdane, N., Derraz, H. T., Mathieu, C., Khelifa, B., and Desfeux, R., 2003, "Effect of substrate temperature on the structural and optical properties of MoO_3 thin films prepared by spray pyrolysis technique, " Materials science and Engineering B, 97, pp. 5-8.
18. Ganguly, A., and George, R., 2007, "Synthesis, characterization and gas sensitivity of MoO_3 nanoparticles, " Bull. Mater. Sci., 30, pp. 183-185.
19. Patil, P. R., andPatil, P. S., 2001, "Preparation of mixed oxide MoO_3-WO_3 thin films by spray pyrolysis technique and their characterization, " Thin Solid Films, 382, pp. 13-22.

20. Stankova, N. E., Atanasov, P. A., Stanimirova, T. J., Dikovska, A. O., andEason, R. W., 2005, "Thin (0 0 1) tungsten trioxide films grown by laser deposition, " Applied Surface Science, 247, pp. 401-405.
21. Yamamoto, S., Inouye, A., and Yoshikawa, M., 2008, "structural and gasochromic properties of epitaxial WO_3 films prepared by pulsed laser deposition, " Nuclear Instruments and Methods in Physics Research B, 266, pp. 802-806.
22. Tagtstrom, P., and Jansson, U., 1999, "chemical vapour deposition of epitaxial WO_3 films, " Thin Solid Films, 352, pp. 107-113.
23. Lee Y. J., Park C. W., Kim D. G., Nichols, W. T., Oh, S. T., and Kim, Y. D., 2010, "MoO_3 thin film synthesis by chemical vapor transport of volatile $MoO_3(OH)_2$, " J. Cer. Processing Resea, 11, pp. 52-55.
24. Gesheva, K. A., Ivanova, T., Popkirov, G., andHamelmann, F., 2005, "Optoelectronic properties of CVD MoO_3 and MoO_3-WO_3 films and their applications in elecrochromic cells, " Journal of Optoelectronics and Advanced Materials, 7, pp. 169-175.
25. Maruyama, T., and Arai, S., 1994, "Electrochromic properties of tungsten trioxide thin films prepared by chemical vapour deposition, " J. Electrochem. Soc., 141, pp. 1021-1024.
26. Hamelmann, F., Gesheva, K., Ivanova, T., Szekeres, A., Abrahev, M., andHeinzmann, U., 2005, "Optical and elecrochromic characterization of multi-layered mixed metal oxide thin films, " Journal of Optoelectronics and Advanced Materials, 7, pp. 393-396.
27. Poniatowski, E. H., Jouanne, M., Morhange, J. F., Julien, C., Diamant, R., Guasti, M. F., Fuentes, G. A., and Alonso, J. C., 1998, "Micro-Raman characterization of WO_3 and MoO_3 thin films obtained by pulsed laser irradiation, " Applied Surface Science, 127-129, pp. 674-678.
28. Gesheva, K., Szekeres, A., and Ivanova, T., 2003, "Optical properties of chemical vapour deposited thin films of molybdenum and tungsten based metal oxides, " Solar energy Materials and Solar cells, 76, pp. 563-576.
29. Rougier, A., Portemer, F., Quede, A., and Marssi, M. E., 1999, "Characterization of pulsed laser deposited WO_3thin films for electrochromic devices, " Applied Surface Science, 153, pp. 1–9.
30. Deepa, M., Kar, M., andAgnihotry, S. A., 2004, "Electrodeposited tungsten oxide films: annealing effects on structure and electrochromic performance, " Thin Solid Films, 468, pp. 32–42.
31. Srivastava, A. K., Deepa, M., Singh, S., Kishore, R., and Agnihotry, S. A., 2005, "Microstructural and electrochromic characteristics of electrodeposited and annealed WO_3 films, " Solid State Ionics, 176, pp. 1161-1168.
32. Nirupama, V., and Uthanna, S., 2010, "Influence of sputtering power on the physical properties of magnetron sputtered molybdenum oxide films, " J. MaterSci: Mater Electron., 21, pp. 45-52.
33. Uthanna, S., Nirupama. V., and Pierson, J. F., 2010, "substrate temperature influenced structural, electrical and optical properties of dc magnetron sputtered MoO_3 films, " Applied Surfacescience, 256, pp. 3133-3137.

34. Atuchin, V. V., Gavrilova, T. A., Kostrovsky, V. G., Pokrovsky, L. D., and Troitskaia, I. B., 2008, "Morphology and structure of hexagonal MoO_3nanorods, " Inorganic Materials, 44, pp. 622-627.
35. Ivanova, T., Gesheva, K. A., Popkirov, G., Ganchev, M., andTzvetkova, E., 2005, "Electrochromic properties of atmospheric CVD MoO_3 and MoO_3-WO_3 films and their application in electrochromic devices, " Materials Science and Engineering B, 119, pp. 232-239.
36. Bai, H. X., Liu, X. H., and Zhang, Y. C., 2009, "Synthesis of MoO_3nanoplates from a metallorganic molecular precursor, " Materials Letters, 63, pp. 100-102.